Particle and Field Signatures of Coronal Mass Ejections in the Solar Wind

Marcia Neugebauer and Raymond Goldstein

Jet Propulsion Laboratory, California Institute of Technology, Pasadena, CA

Short Title: Interplanetary Signatures

Abstract. When CME plasma passes over a spacecraft in interplanetary space, it can often be recognized by a number of characteristic signatures in the properties of the plasma and magnetic field. Those signatures are briefly summarized. When two or more signatures are present, they are, often not synchronized with each other. As an example., the low-temperature signature is often encountered ahead of the bidirectional streaming of suprathermal electrons. Periods of quiet, nearly radial fields are found in the trailing portions of approximately one quarter of the fast or energetic CME events. It is suggested that the radial fields may be manifestations of the legs of magnetic loops carried into space by the CME. Another feature of the trailing portions of some CME events is a strong flux of outward propagating Alfvén waves. in some events these waves probably represent a return to the ambient solar wind through which the CME is propagating, but we suggest that in other events the waves may be a signature. of a transient mend hole at the footpoints of the CME.

'1'here is no single distinctive feature exhibited by all CME-generated plasma in the solar wind. Rather, the identification of CMEs in the interplanetary medium must rely on several features that may appear singly or jointly with other features in any particular event. What are those features or CM] ; signatures?

(1) Unusuall y low kinetic temperatures of icms and/or electrons for a given solar-wind speed. In the quasi-stationary solar wind, ion temperatures are positively correlated with flow speed. Figure 1 showsa scatter plot of proton temperature versus speed for intervals of known flow type - open symbols (squares, circles, or triangles) for quasi-stationary flows and line symbols (x, -1 or -) for CME flows observed by ISEE 3. The method of event selection and identification is explained in a paper by *Neugebauer and Alexander [1991].* The principal points are that (a) most of the open symbols arc above the diagonal line while most of the lined symbols are below it, and (b) there are quite a few exceptions. We have defined a "thermal index" I_{th}, by

$$I_{th} = (500 v_p - 11.75 \times 10^5)/f, \quad (1)$$

which is >1 for points below the line and <1 for points above it, With a significant number of exceptions, if/h >1, the plasma is likely to be associate.d with a CME. This method of identifying CME plasma is qualitatively similar to the method developed and used by *Richardson and Cane* [199S] and others. The cause of the low temperature or high thermal Mach number of CME plasma in the solar wind is probably the 3-dimensional expansion of the transient plasma cloud into the ambient solar wind. In contrast, under quasi-

stationary conditions, the flow is channeled and expansion is limited to the areal expansion rate of the flow tubes from the Sun. This effect is illustrated by the. cartoon in Figure ?.

(2) An unusually pronounced anisotropy of the proton distribution with $T_{\parallel} > "]"$,, caused by the conservation of the magnetic moment of the ions as the plasma expands.

(3) Unusually high helium abundance. If the ratio of the. number density of helium n_{α} to that of protons n_p exceeds ~0.08, the plasma is almost certainly either in or near an interplanetary cloud generated by a CME. The cause of the helium enhancements has not yet been established theoretically. One possibility is that it is a sludge removal phenomenon wherein helium left behind at the base of the flow tubes, especially those in the slow wind near the heliospheric current sheet, is cleaned out by the explosive event. This CME signature is often patchy within an event or entirely missing.

(4) Anomalies in the abundances of other ion species. This topic is reviewed in the paper by Galvin (this volume).

(5) Bidirectional streaming of suprathermal electrons and energetic ions. This feature is considered to be. indicative of a closed magnetic configuration with bet]) footpoints of the field lines rooted in the Sun. in this volume, these features arc discussed in papers by Gosling (for electrons) and by Richardson (for energetic ions).

(6) Quiet, strong magnetic fields which, when combine.ci with the low temperatures, leads to low β. in CME plasma, the proton β is often less than 0.1.

(7) Rotations of the magnetic field that can be modeled as flux ropes. Some of these Configurations qualify to be called "magnetic clouds" if the field strength increases by a factor >2., at least one component of the field has a large, smooth rotation, and the ion temperature is low. Magnetic clouds and flux ropes are discussed further in the papers by Osherovich and by Gosling (this volume), respectively.

(8) Decrease in the flux of low energy cosmic rays, This topic is also covered in this volume in a paper by Richardson.

(9) Unusual ionization states of heavy ions, indicative of a plasm source in either hot coronal loops or (very occasional y) in relatively cold prominence material. See the paper by Galvin (this volume) for further discussion.

To this list of CME signatures, wc can add other features that are associated with the more energetic events that result in plasma flows significantly faster than the ambient, quasi-stat ionary solar wind. These feat ures include a forward shock ahead of the pl asma cloud, a sheath of compressed, noisy plasma between the shock and the cloud, the draping of the interplanetary magnetic field around the cloud, and local maxima (sometimes spikes) in the pressure and density at the cloud's leading edge.

Figure 3 illustrates some. of the signatures and features discussed above for a CME event observed by ISEE 3 on days 232-234 (Aug 2,()-22,), 1979. The event started with an interplanetary shock denoted by the vertical line labeled S. The sheath, with its increased temperature, densit y, pressure, and field st rength, is shown between the shock and the discontinuity 1)1, where the spacecraft entered the CME cloud. Note the spike in proton densit y at 1 D 1 and the start of an interval of high helium abundance (n_α/n_p) anti a high value of the thermal index I_{th}. The hori zontal bar in the top panel denotes the interval of bidirectional streaming of suprathermal electrons (J. '1'. Gosling, personal communication). This event did not contain a magnetic cloud. If the CME plasma is assumed to extend from D1 to D3, where I_{th} is high, the. patchiness of the, helium abundance enhancements is quite evident.

Since not all the CME signat ures are synchr onized with each other, some appearing at different times than others or not at all, it is interested to determine if there are any significant temporal patterns. We are currently studying this question and can show only a

few preliminary results here. Figure 4A shows a superposed epoch histogram of the fraction of each hour that bidirectional streaming of suprathermal electrons was observed by ISEE 3 (based on the data in the list given by *Gosling et al.* [1987]) where the zero epoch is the hour in which the bidirectional streaming stared. It is seen that the duration of bidirectional electron streaming is typically 8 to 10 hours. Figure 4B shows the fraction of hours with I_{th} >1 as a function of time before and after the same mro-epoch times as in Figure 4A. It is clearly seen that the I_{th} >1 indicator extends for ~2 days after the zero epoch, thus lasting much longer than the bidirectional electron streaming. This pattern is consistent with the field lines in the CME plasma reconnecting with the ambient field in the manner postulated by *Gosling et al.* [19950].

The horizontal line in figure 4B represents the fraction of all hews for which ISEE 3 velocit y and temperature were available and for which $I_{th} > 1$; i e,., on average, I_{th} exceeds unity 6.4% of the time. It is probably significant that I_{th} *is* greater than average for the. day preceding the zero epoch time at which the bidirectional streaming starts. in many individual events, intervals of $I_t > 1$ arc seen before the appearance of bidirectional streaming. Figure 4C shows a histogram similar to those in Figures 4A and 4B, except that the zero epoch time is chosen as the start of I_{th} >1. In panel 4C, it can be seen that the bidirectional electron streaming generally starts ≥10 hours into the, CME as identified by I_{th} >1. This result suggests that the fields at the leading edge or the nose of the CME cloud tend to be reconnected to the interplanetary field. This is not surprising because it is at the nose where the CME and interplanetar y fields are most strongly pressed together, at least for' that part of its trajectory where the. CME is faster than the ambient wind.

One feature of fast CMEs that has not been previously reported is the appearance of extended intervals of quiet radial fields in their trailing edges. 1 figure 3 contains an example. of this phenomenon; the next to bottom panel shows that B_x/B, where B_x is the radial

component of the field in heliographic solar ecliptic coordinates, was close to -1 between D2 and D4 (days 233.8-234.7). We have found intervals with $|B_x|/B > 0{,}9$ for ≥6 consecutive hours in the trailing portions of about one quarter of the major CMEs observed by 1S1 :E 3. About half the time, the quiet, radial fields overlapped other CME signatures such as high n_α/n_p, high I_{μ}, or bidirectional streaming (as in Figure 3), and the rest of the time. they immediately followed those signatures. in every case, the CME speed was greater than the ambient wind speed and the quiet radial field was observed during a period of strongly decreasing solar wind speed. None of the radial-field events occurred in a CME that had been designate.d as a magnetic cloud by *Zhang and Burlaga* [1988]. We suggest that a ~M}i-associated quiet radial field interval may mean the spacecraft is situated in a leg of a magnetic loop (or perhaps even a flux rope.) whose leading edge has been stretched out into space by the fast plasma at the front of the cloud. A paper presenting further information on the possible x-elation of quiet radial fields to the legs of magnetic loops is in preparation,

Next, consider the bottom panel of Figure 3 which shows a plot of the normalized cross helicity σ_c

$$\sigma_c = \frac{2 < \delta v \cdot \delta B >}{< \delta v^2 + \delta B^2 >} \qquad (2)$$

where the sign of σ_c has been "corrected" for the sector structure such that $\sigma_c = +1$ indicates Alfvén waves propagating outward from the Sun along the magnetic field. The values of σ_c were, calculated from the variations of 5-minute values of velocity v and magnetic field B over periods of 2.4 hours. Figure 3 shows an extended period of high σ_c starling at D4 (where the quiet radial field ended) and persisting for over a day. Outward

propagating Alfvén waves are prevalent in high-sped flow from coronal holes, and may be remnants of the wave field responsible for the acceleration of the wind in an open-fic]d geometry. Wc therefore speculate that the waves seen cm day 235 may have originated in a transient coronal hole. created by the eruption of the. CME. Examples of such transient coronal holes were shown in the poster paper presented by *Webb et al.* at this conference. They arc interpreted as the footpoints of flux rope.s evacuated by the CME. Similar intro vals of intense wave activity can be found behind many CMEs, but there is a question whether they indicate a CME-associated feature or re-entry into the ambient solar wind, For the particular event shown in Figure 3, we believe the Alfvénic wave flux is part of the CME because (1) it occurs on the velocity gradient caused by the CME and (2) in the quasi-stationary wind, Alfvénic fluctuations are not commonly found at solar wind speeds as low as the -400 km/s average speed observed during, this particular Alfvénic event,

Almost everything discussed above has been based on the properties of CMEs observed near the ecliptic plane. There are both a number of similarities and some impor tant differences between the CMEs described above and those studied at high latitudes by Ulysses. The similarities include the decreased ion temperatures, bidirectional streaming, and occasional flux ropes, magnetic clouds, and quiet radial field intervals. It is the differences that arc more interesting. First, each of the high-latitude CME plasma clouds had roughly the same speed (>700 km/s) as the ambient quasi-stationary solar wind from the polar coronal holes [*Gosling et al.*, 1994n]. This finding may man that, except for the most energetic CME events, once the CME plasma is released from the Sun, the same processes accelerate the transient and quasi-stationary winds. At low latitudes, where the ~h411 plasma is embedded in slow solar wind, the magnetic field in the plasma cloud is strong and steady, showing little evidence for Alfvénic fluctuations, but the CME clouds in the fast, high-latitude wind are just as Alfvénic as the ambient plasma, suggesting an

important role for wave acceleration of the high-latitude CME plasma. *Gosling and Riley [1996]* suggest that the acceleration of the CME plasma may be caused by the dynamic interaction of the slower plasma cloud with the higher-speed ambient wind ahead of and behind it.

If the high-latitude CMEs have nearly the same speed as the ambient high-latitude wind, one might not expect the n to be preceded by an interplanetary shock. in fact, however, many of the high-latitude, CMEs are observed to be preceded by a forward shock and followed by a reverse. shock [*Gosling et al.*, 1994*b*]. The driver for these shocks (or rather for- a single 3-1) shock that crosses the spacecraft twice.) is the rapid expansion of the CME into the surrounding plasma rather than its overtaking slower plasma in its path.

Another departure. of high-latitude CMEs from the typical behavior near the ecliptic is the absence of helium abundance enhancements. As reported by Galvin (this volume.), the differences in ionization charge states between CMEs and quasi-stationary plasma is also smaller at high latitudes than near the ecliptic.

Gosling et al. 11995b] have compared the properties of a single CME observed by both IMP 8 near Earth and Ulysses at 54°S and a heliocentric distance of 3.5 AU. in addition to the differences discussed just above, this comparison shows that because of the higher speed at high latitude, the instantaneous shape of the. plasma cloud must be very different from the, familiar sketches or cartoons of(;h41 s.

Acknowledgments. We thank Doug Clay for his contribution to the compilation of the relative timing of different CME features. This research was performed at the Jet Propulsion Laboratory under a contract between tile.'!:alifomia Institute of Technology ant] the National Aeronautics anti Space Administration.

REFERENCES

Gosling, J. 'I'., D. N. Baker, S. J. Bame, W. C. Feldman, R. D. Zwickl, and E. J. Smith, Bidirectional solar wind electron heat flux events, *J. Geophys. Res.*, 92,8519, 1987.

Gosling, J. "l'., S. J. Bame, D. J, McComas, J. L. Phillips, B. E. Goldstein, and M. Neugebauer, The speeds of corona] mass ejections in the solar wind at mid heliographic latitudes: Ulysses, *Geophys. Res. Lett., 21, 1109,* 1994*a*.

Gosling, J, T., J. Rim, and M, Hesse, Three-dimensional magnetic reconnection and the magnetic topology of coronal mass ejection events, *Geophys. Res. Lett.*, 22, 869, 19956',

Gosling, J. '1'., D. J. McComas, J. E. Phillips, L. A. Weiss, V. J. Pizzo, 11.11. Goldstein, ant] R. J. Forsyth, A new class of forward-r-c.verse shock pairs in the solar wind, *Geophys. Res. Lett., 21*, 22-?1, 1994*b*.

Gosling, J. 'l'., D. J. McComas, J. L. Phillips, V. J. Pizzo, B. E. Goldstein, R, J. Forsyth, and R. P. Lepping, A CME-driven solar wind disturbance observed at both low ant] high heliographic latitudes, *Geophys. Res. Lett., 22*, 1753, 1995 b.

Gosling, J. 'l'., and 1'. Riley, The acceleration of slow coronal mass ejections in the high-speed solar wind, *Geophys. Res. Lett.*, 2.?, in press, 1996.

Neugebauer, M., and C. J. Alexander, Shuffling footpoints and magnetohydrodynamic discontinuities in the solar wind, *J. Geophys. Res., 96, 9409,* 1991.

Richardson, I. G., and 11, V. Cane, Regions of abnormally low proton temperature in the solar wind (1965-1991) and their association with ejecta, *J. Geophys. Res., 100,* 23397, 1995.

Zhang, G., and 1., F. Burlaga, Magnetic clouds, geomagnetic disturbances, and cosmic ray decreases, *J. Geophys. Res., 9.?, 2511,* 1988.

FIGURE CAPTIONS

Fig. 1. Scatter plot of proton temperature versus proton speed for intervals clearly identified as flow associated with either coronal holes (CH), interstream (1 S), heliospheric plasma sheet (1'S), bidirectional electron streaming (BES), helium abundance enhancements (HAE), or magnetic clouds (MC). The line is the trace of equation (1) for I_{th} = 1.

Fig. 2. A cartoon depicting the difference in the modes of expansion of the channeled flow in the quasi-stationary wind and the 3-dimensional expansion of CMEs.

Fig. 3. From top to bottom, the parameters plotted are proton speed, proton temperature, proton density, the ratio of the alpha-particle to proton densities, the total gas plus magnetic pressure in the plasma frame, an index I_{th} defining the relation between proton temperature and speed as defined in Equation (1), the magnetic field strength, the ratio of the radial component of the field divided by field strength, and the normalized helicity as defined by Equation (2). Each plasma data point is a 5-minute sample and each field data point is a 5-minute average.

Fig. 4. Histograms of the frequency of detection of bidirectional streaming of suprathermal electrons (BDES) and of the occurrence thermal index $I_{th} > 1$ in a superposed epoch format. (A) Frequency of detection of BDES as a function of time from a zero epoch defined by the. first detection of BDES. (B) Frequency of $I_{th} > 1$ with zero epoch defined by start of BDES. (C) Frequency of BDES with zero epoch defined by start of $I_{th} > 1$.

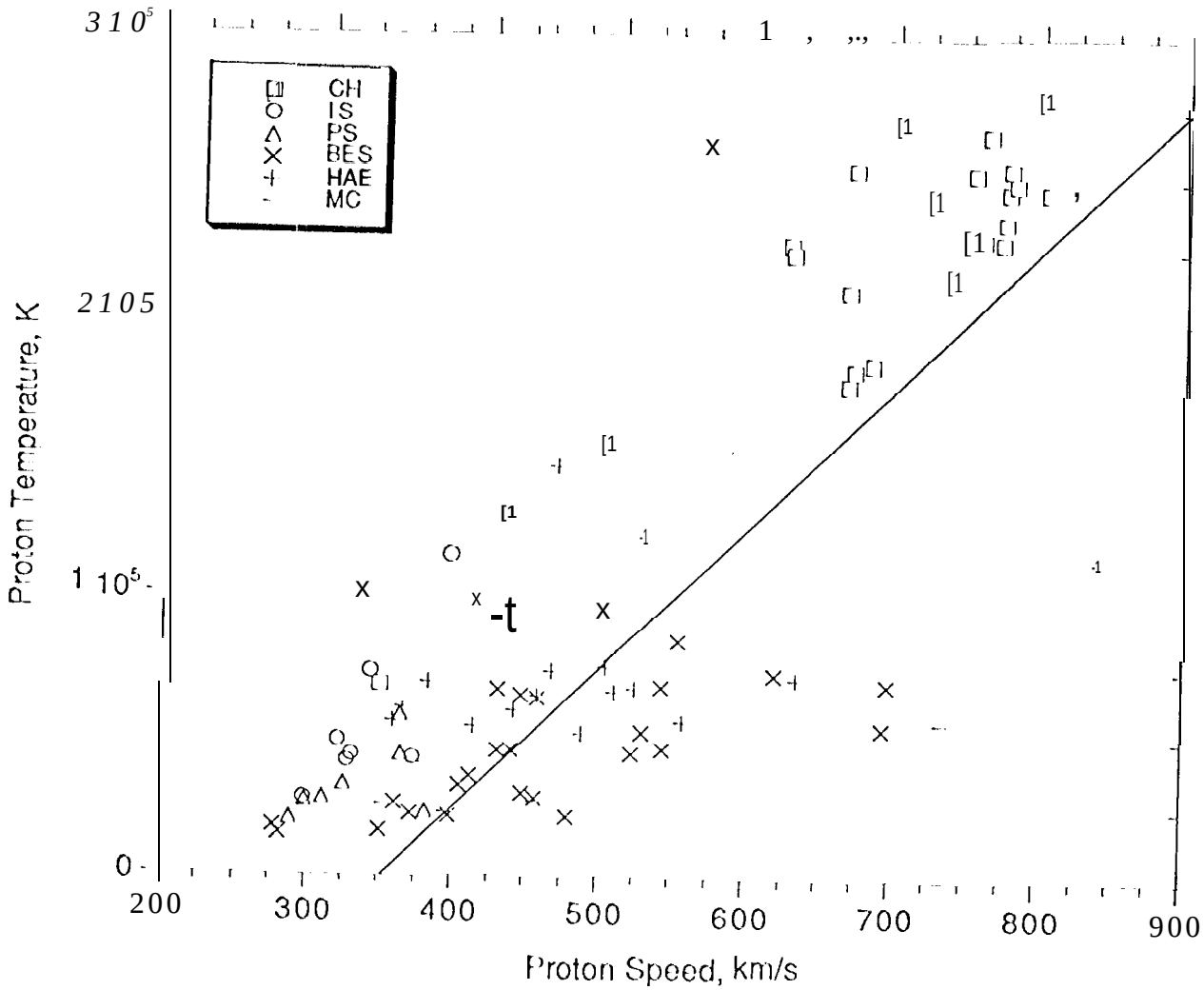
CH
IS
PS
BES
HAE
MC
Proton Temperature, K
Proton Speed, km/s
200
300
400
500
600
700
800
900
0
2105

Fig. 1

Coronal Hole

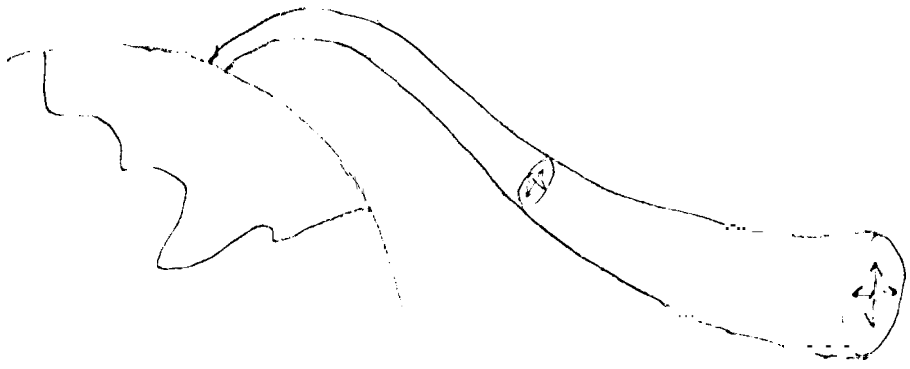

Coronal Mass Ejection

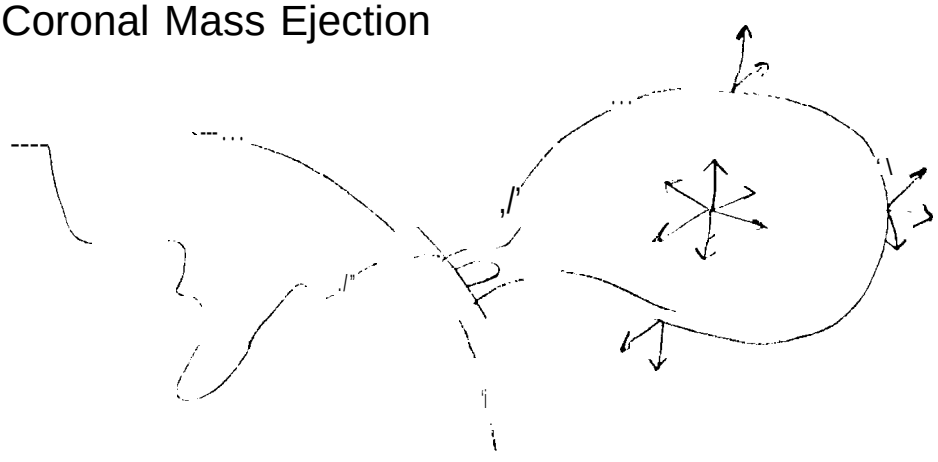

Fig 2

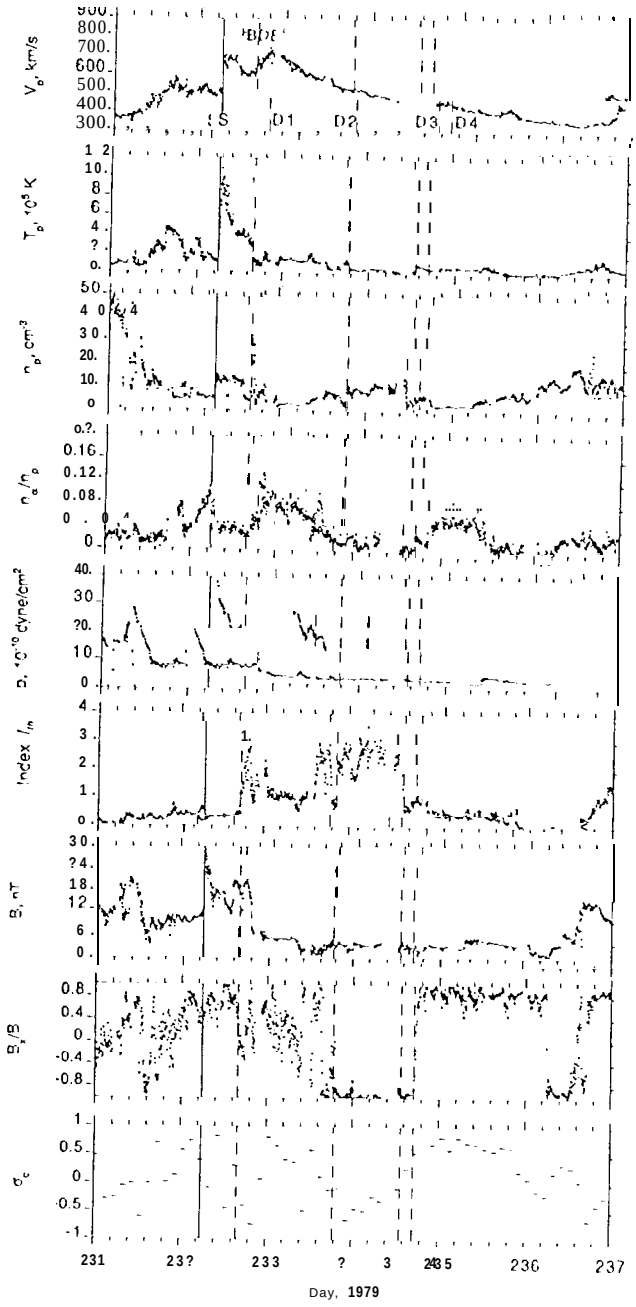
V_p, km/s
T_p, 10^5 K
n_p, cm^{-3}
n_α/n_p
P, 10^{-10} dyne/cm^2
Index I_m
B, nT
B_x/B
σ_c
S
D1
D2
D3
D4
231
232
233
234
235
236
237
Day, 1979

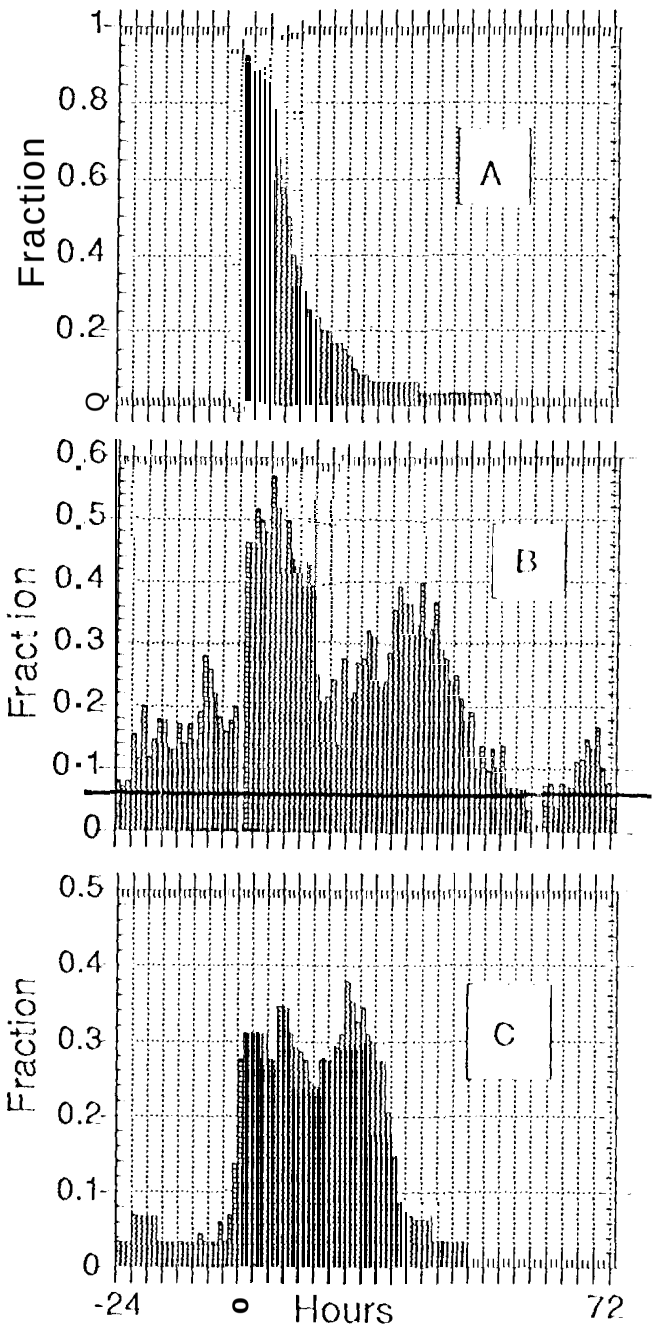
Fraction
1
0.8
0.6
0.4
0.2
0
A
Fraction
0.6
0.5
0.4
0.3
0.2
0.1
0
B
Fraction
0.5
0.4
0.3
0.2
0.1
0
C
-24
0
Hours
72

Fig 1